A semi-empirical model for stress relaxation including primary and secondary creep stages

J. K. SOLBERG*
Central Institute for Industrial Research, Blindern 0314, Oslo 3, Norway

A universal creep law which incorporates both primary and secondary creep has been used to develop a semi-empirical model for stress relaxation. The modelling was performed by comparing computer simulated relaxation curves with experimental data. Contrary to most models for stress relaxation, the results indicate that relaxation life should be divided into two stages, a primary stage with increasing internal stress and a secondary stage during which the internal stress falls as the applied stress decreases.

1. Introduction

Stress relaxation is frequently expressed mathematically through an Arrehnius-type of rate equation [1]

$$\sigma = -c\varrho \exp(-Q/kT) \exp\left[\frac{v(\sigma - \sigma_i)}{kT}\right] \quad (1)$$

where σ is the applied (remaining) stress, σ_i the friction stress, c a constant including some mathematical parameters, ϱ the density of mobile dislocations, Q the activation energy, k Boltzmann's constant, T the absolute temperature, and v a quantity called the activation energy. If c, ϱ and v are assumed constant during a test, and σ_i is neglected or assumed constant, integration of this equation leads to an expression of the following form for σ as a function of time t [1]

$$\sigma = \sigma_0 - \frac{kT}{v}\ln\left(1 + \frac{t}{t_0}\right)$$
$$\frac{1}{t_0} = \frac{vc\varrho}{kT}\exp\left(\frac{Q - v\sigma_0}{kT}\right) \quad (2)$$

where σ_0 is the applied stress at $t = 0$.

Equation 2 predicts a linear relationship between σ and log time, and references to several investigations are given in [1] which have shown that a plot of σ against log time after a short initial period turns into a straight line. However, the tests described in those papers have only been carried out at relatively short periods of time. Both the long-range tests performed by Herø [1] and the experiments done in this work have given a non-linear relationship between σ and log time. The reason for this may be changes occurring in the microstructure of the specimens during the tests. Herø [1] has suggested that the mobile dislocations are gradually arrested by obstacles. If no dislocation multiplication or reactivation takes place, the internal stress σ_i will therefore increase. He suggests that this increase is proportional to the strain in the stress relaxation process, i.e. that the internal stress varies linearly with the decrease in σ. In this respect he considers stress relaxation as a primary creep process. This is in contradiction to the case described by Equation 2 where a kind of steady state creep is assumed. In this work the variation in the internal stress with the applied (remaining) stress has been taken into consideration in a mathematical simulation of stress relaxation. As in the development of Equations 1 and 2, we have assumed that stress relaxation is a pure creep phenomenon. Contradictory to the former case, however, we have allowed σ_i to vary as a function of time and stress. Both primary and secondary creep are included in the mathematical model.

2. General description of the model for stress relaxation

The model is based on an equation for secondary creep rate $\dot{\varepsilon}_s$ developed by Evans and Harrison [2]

$$\dot{\varepsilon}_s = B\left(\frac{\sigma - \sigma_i}{\sigma_{0.05}}\right)^{3.5} \quad (3)$$

where $B = 2.5 \times 10^{-5}\,\text{sec}^{-1}$, σ is the applied stress, σ_i is the internal friction stress opposing creep, and $\sigma_{0.05}$ is the 0.05% proof stress. The equation was originally developed for iron and nickel alloys, but was suggested by the authors to be of universal validity. In a recent work by Solberg and Thon [3] Equation 3 was shown to be valid for some aluminium alloys, including AlSi12 (Al–12 wt % Si) which we have used to illustrate the present model for stress relaxation. In this model, the Evans–Harrison creep equation (Equation 3 above) is assumed to be valid for each value of the remaining stress during the relaxation test. The internal stress is then the only unknown quantity which must be determined to evaluate the strain rate at each stress value. The variation in σ_i during a stress relaxation test is not trivial to determine, however. In this model we have assumed that σ_i increases at the beginning of the test, just as it does during primary creep. However, after a well-defined subgrain structure (characteristic of secondary creep) has developed, it is assumed that the

*Present address: Physical Metallurgy, Technical University of Trondheim, 7034 Trondheim – NTH, Norway.

0022–2461/86 $03.00 + .12

internal friction decreases as the applied stress decreases. It is assumed that this fall in σ_i is associated with an increase in the subgrain size. By this procedure we use the Evans–Harrison creep equation to describe stress relations as successive primary and secondary creep processes. It is true that the equation was originally developed for secondary creep. However, in a later paper [4] the authors show that the equation is valid for initial creep ($t = 0$) if the internal friction stress at this stage is inserted. On this background the equation can be used for the whole stress relaxation test.

3. Mathematical derivation of an equation for stress relaxation

During a stress relaxation test the specimen is strained to a strain value ε_t which remains constant during the test. At $t = 0$ ε_t is only the elastic strain ε_e. As time passes the elastic strain is gradually transformed to plastic strain, ε_p. We therefore have

$$\varepsilon_t = \varepsilon_e + \varepsilon_p = \text{constant}$$

where ε_p increases with time, resulting in a reduction in the applied stress. At each stress level, ε_e is equal to σ/E, E being the Young's modulus of elasticity. We therefore obtain

$$\frac{\sigma}{E} + \varepsilon_p = \text{constant}$$

which upon derivation with respect to time gives

$$\frac{1}{E}\frac{d\sigma}{dt} = -\dot{\varepsilon}_p$$

Here $\dot{\varepsilon}_p$ is the creep rate at each value of the remaining stress σ. Substituting Equation 3 for $\dot{\varepsilon}_p$ gives

$$\frac{d\sigma}{dt} = -EB\left(\frac{\sigma - \sigma_i}{\sigma_{0.05}}\right)^{3.5} \quad (4)$$

where $\sigma_i = \sigma_i(t, \sigma)$ is a complicated function of time and stress. Equation 4 gives the slope of the curve of stress against time.

To obtain an expression for the variation of σ with time, Equation 4 should have been integrated. However, since we will allow σ_i to take any complicated form, such an integration may be impossible to carry out. Equation 4 must therefore be used as it stands, and the mathematical simulation of the stress relaxation process has to be performed numerically by means of a computer.

4. Model for the variation in internal stress

To calculate the remaining stress as a function of time a model for the variation of σ_i during stress relaxation must be developed. Following the ideas outlined in the previous section, we divide the relaxation process into two stages. At $t = 0$ all dislocations are mobile, and the friction force is low. As in creep the dislocations will be rearranged, and a higher internal stress will build up. At a remaining stress of σ_p the dislocation rearrangement is thought to be complete. It is assumed that the internal stress at this point equals the

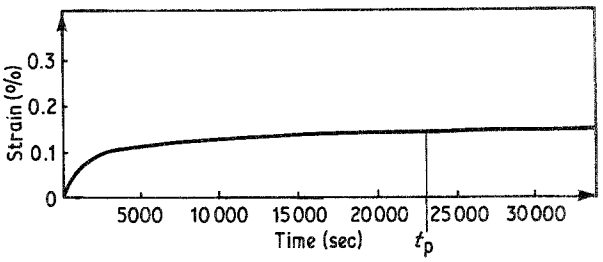

Figure 1 Creep of ÅSV 3001 at 100° C at a stress of 88.8 MPa. End of primary stage at $t_p = 23\,000$ sec.

internal stress during steady state creep at an applied stress of σ_p. This point defines the transition from the primary stage to the secondary stage. During the latter stage, the dislocations are again assumed to be rearranged as the applied stress falls. However, it is not likely that the rearrangement develops with the same speed as the fall in the applied stress. During the secondary stage, the friction force may therefore be higher than during steady state creep at corresponding stress levels.

We must first obtain a model for the variation in σ_i during the primary stage. Evans and Harrison [4] have suggested a method for finding the friction stress at $t = 0$. They extrapolate the σ_i against σ graph so that it intersects the σ_i axis at $\sigma = 0$. The σ_i value given by the point of intersection is taken to be the friction stress at $t = 0$ during a creep test. By using this method a much too high relaxation rate was calculated in the initial stage in the present case, so we have chosen another approach which estimates the internal stress from primary creep data. The method was carried out for the concrete case of stress relaxation of ÅSV 3001 at 100° C and an initial stress of 88.8 MPa. The alloy was delivered by Årdal and Sunndal Verk a.s., Norway, and had the composition (in wt %) Al–11.92Si–0.18Fe.

First, a creep curve for corresponding experimental conditions was obtained by means of an extensiometer attached to a specimen of diameter 5 mm and gauge length of 40 mm, Fig. 1. The primary creep rate was then measured for several points along the creep curve, and the corresponding σ_i values were calculated from Equation 3, assuming that the equation is valid for the primary stage. In a log–log plot of σ_i against time the calculated values turned out to lie along a straight line, as shown in Fig. 2. The straight line gives the following equation for σ_i with respect to time, t

$$\sigma_i = Ct^m \quad (5)$$

$C = 36.6$ MPa, $m = 0.08$. The expression is valid till the end of the primary creep stage, $t = t_p = 23\,000$ sec, where σ_i takes the constant value characteristic of the secondary stage. In Fig. 3 this development of σ_i is sketched by the upper left curve. The right-hand diagram gives the internal stress for secondary creep, σ_i^s, as a function of applied stress (curve (a)). At the creep stress σ_0 this value is equal to σ_{i0}^s. Fig. 4 gives the σ_i against σ curve for secondary creep of ÅSV 3001 at 100° C as determined by Solberg and Thon [3].

It is now assumed that the creep expression of

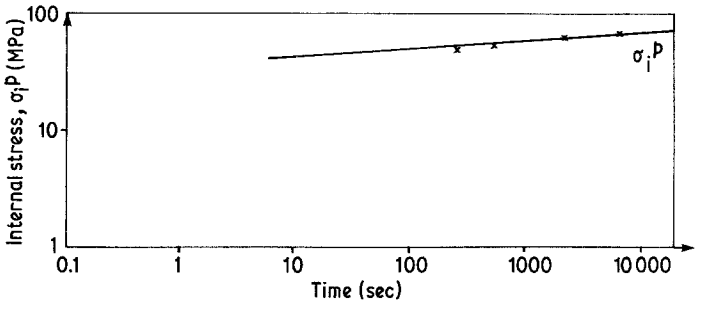

Figure 2 The variation of internal stress with time during the primary creep stage of Fig. 1.

Equation 5 holds during the first infinitesimal time interval dt of a stress relaxation test which starts at the same load σ_0 as the creep load. During the time interval dt the applied stress falls to a value σ_1. For creep, the secondary stage value of the internal stress corresponding to this stress is equal to σ_{i1}^s, Fig. 3. In the next time interval of the relaxation test, we assume that the internal stress increases towards this value, and not towards σ_{i0}^s. This is visualized by the next upper curve to the left in Fig. 3. This curve is also assumed to have a Ct^m shape, and we assume that the new curve takes the value σ_{i1}^s at the same time t_p as the upper curve takes the value σ_{i0}^s. The values C and m are determined by the known start and end points of the curve

$$m = \log[\sigma_{i1}^s/\sigma_i(t_1)]/\log[t_p/t_1]$$

and

$$C = \sigma_i(t_1)/t_1^m.$$

This sequence is now repeated, so at time $t_2 = 2\mathrm{d}t$ the stress has fallen to σ_2, characterized by an internal creep stress of σ_{i2}^s. The internal stress grows towards this value during the next time interval dt, and so on. Each new curve for the increase in σ_i is assumed to have a Ct^m shape. The resulting internal stress values are drawn with a heavy line.

It is assumed that the primary stage of the stress relaxation test has the same duration t_p as during the creep test. At this time the applied stress has fallen to σ_p, and the internal stress has reached the value σ_{ip}^s which characterizes the secondary creep stage at stress σ_p. From now on the internal stress during stress relaxation will fall simultaneously with the fall in applied stress. In an ideal case the values for the internal stress would follow the σ_i^s against σ curve to the right in Fig. 3 (Curve (a)). However, the internal dislocation structure in a real material will need some time to adjust to a new stress state, so the internal stress during the rest of the relaxation test is likely to lie above the σ_i^s graph in Fig. 3. This is indicated by the line (b) which forks out from the σ_i^s graph at the stress value σ_p. Of course, it is impossible to know the exact shape of this line. For the sake of simplicity, we have in our calculations assumed that the line is straight, and that it crosses the σ_i^s-axis at a value $\sigma_{i\infty}$ which has to be guessed. The corresponding fall in σ_i with time is indicated in the diagram to the left in Fig. 3.

5. Calculations

The numerical calculations were carried out by choosing time intervals dt of 1 sec. During each time interval the internal stress was given a constant value equal to the average of the values at the beginning and end of the interval. The new stress value at the end of each time interval was calculated through three successive steps. This procedure is illustrated for the first time interval in Fig. 5. The exact mathematical relaxation curve is given by the solid line, the initial stress being σ_0. The slope of the curve is given by Equation 4, where σ during the first second is approximated by the average value σ_{iav} for $t = 0$ and $= 1$ sec in Equation 5. This gives the following approximate value for the stress after 1 sec

$$\sigma_1' = \sigma_0 - EB\left(\frac{\sigma_0 - \sigma_{iav}}{\sigma_{0.05}}\right)^{3.5} \times 1\,\mathrm{sec}$$

$$= \sigma_0 - A(\sigma_0 - \sigma_{iav})^{3.5} \times 1\,\mathrm{sec}$$

This value lies below the true curve as shown in Fig. 5. We now take the average stress value

$$\sigma_{av}' = \frac{\sigma_0 - \sigma_1'}{2}$$

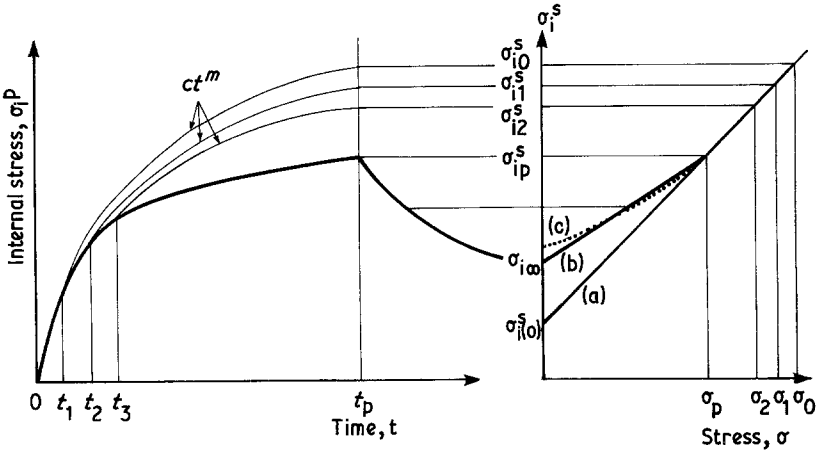

Figure 3 A model for the variation of the friction stress with time during stress relaxation. (a) σ_i for secondary creep, (b) linear reduction of σ_i during secondary stress relaxation and (c) apparently correct σ_i for secondary stress relaxation.

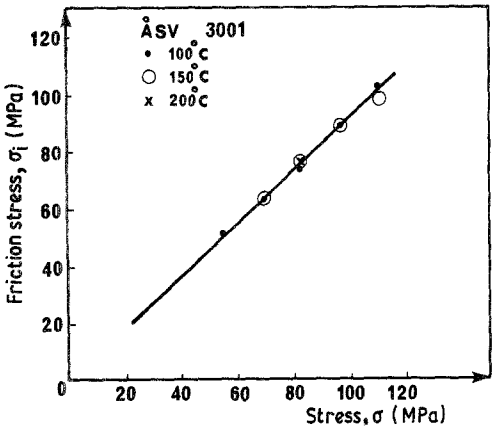

Figure 4 Friction stress as a function of applied stress for ÅSV 3001.

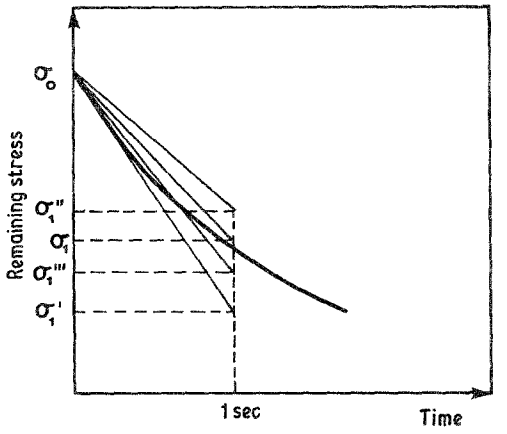

Figure 5 Numerical calculation of the remaining stress after 1 sec. The calculation is made through three successive approximations.

which we put into Equation 4 and calculate a new stress value

$$\sigma_1'' = \sigma_0 - A(\sigma'_{av} - \sigma_{iav})^{3.5} \times 1 \text{ sec}$$

which lies above the true mathematical curve. The average value

$$\sigma''_{av} = \frac{\sigma_0 - \sigma_1''}{2}$$

is then put into Equation 4, giving a new stress value

$$\sigma_1''' = \sigma_0 - A(\sigma''_{av} - \sigma_{iav})^{3.5} \times 1 \text{ sec}$$

which lies below the true curve. Finally, the stress after 1 sec is set equal to

$$\sigma_1 = \frac{\sigma_1'' + \sigma_2''}{2}$$

This value lies slightly above the true value. This sequence is then repeated for each time interval of 1 sec, so the calculated relaxation curve will lie slightly above the true mathematical curve. The deviation from the exact curve is so small, however, that by reducing the number of steps in the approximation from three to two, which gives a calculated curve slightly below the true one, no essential difference in the calculated stress value at the end of the test (10^6 sec) is obtained.

Figs. 6 and 7 give two calculated relaxation curves for ÅSV 3001, using the σ_i against σ relationship given in Fig. 4. The temperature was 100° C and the initial stress 88.8 MPa. The experimental curve is given by the solid line in each diagram, while the calculated curves are shown as dashes. The two calculations differ in the rate at which the internal stress decreases in the secondary stage. The curves are therefore equal up to 23 000 sec, the assumed end point of the primary stage. In Fig. 6 the theoretical relaxation curve for an ideal case is given, i.e., the internal stress during the secondary stage has been assumed to follow the σ_i^s against σ graph in Fig. 3 (i.e., Fig. 4) ($\sigma_{i\infty} = \sigma_{is}(0) = 3$ MPa). It is seen that this results in a much too high relaxation rate in the secondary stage, so the internal stress has been estimated too low. For the calculated curve in Fig. 7, the $\sigma_{i\infty}$ value in Fig. 3 has been set equal to 13 MPa, and this reduces the calculated relaxation rate so that it is much closer to the experimental value. The shape of the calculated curve in the secondary stage is slightly wrong, however. During the first part of this stage, the relaxation rate is lower than the experimental rate, while it is higher in the last part. This suggests that the internal stress in the secondary stage does not vary linearly with the remaining stress as assumed in Fig. 7 and indicated by the thin line in the diagram to the right in Fig. 3. The

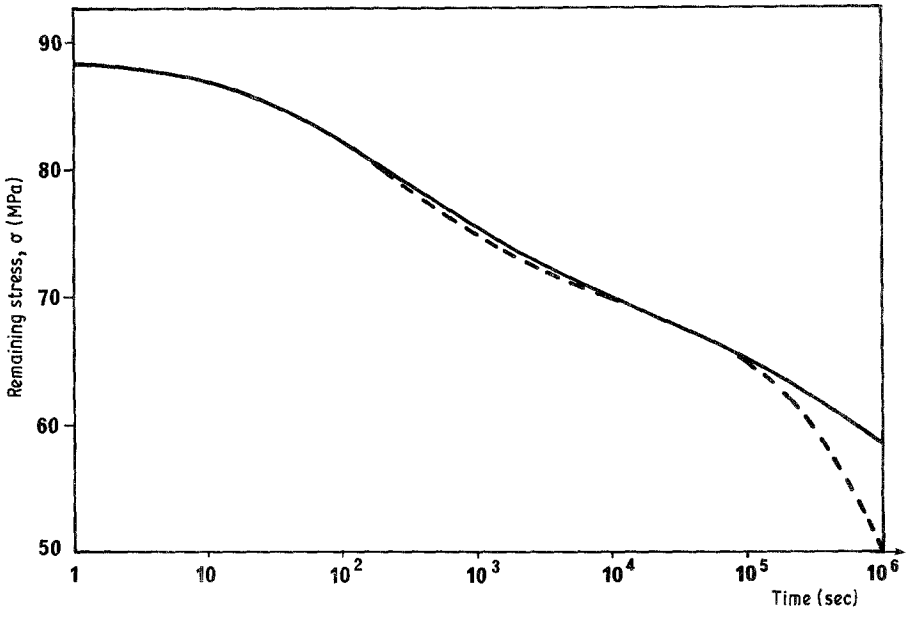

Figure 6 Experimental and calculated remaining stress as a function of time for AlSi12 at 100° C. (———) experimental, (- - -) calculated $\sigma_{i\infty} = \sigma_i^s(0) = 3$ MPa.

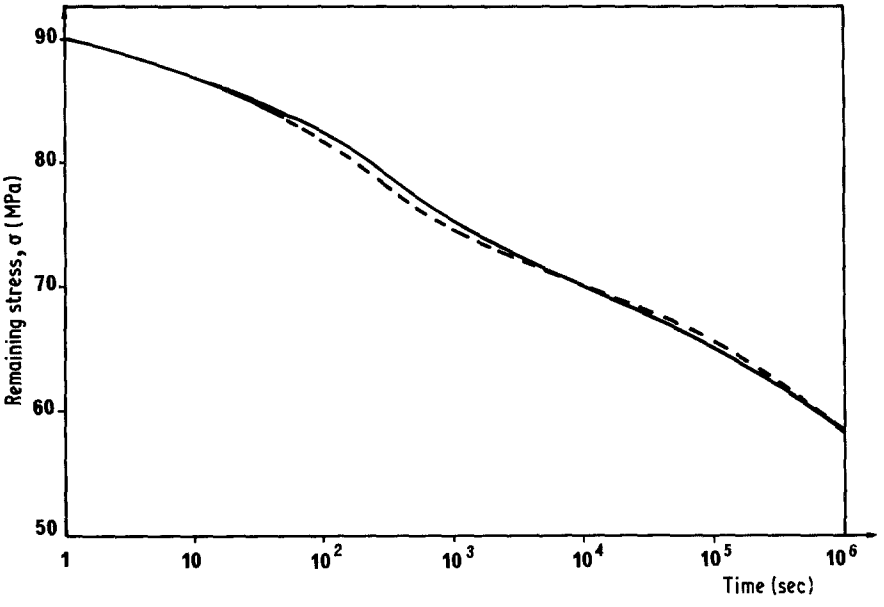

Figure 7 Experimental and calculated remaining stress as a function of time for AlSi12 at 100° C. (———) experimental, (- - -) calculated. $\sigma_{i\infty} = 13$ MPa.

actual internal stress seems to lie closer to the σ_i^s against σ graph during the first part of the secondary stage and further away from this graph in the last part of the stage, shown by the dotted curve in Fig. 3. No attempt at calculating the exact position of the dotted curve has been made since that would only have been a curve-fitting exercise which would have given no addition information of interest.

Of course, the inaccuracy in the experimental internal stress values for the two creep stages affects the calculated relaxation curves. Fig. 8 shows that a very good correspondence between the experimental and calculated curves can be obtained by a slight modification of the σ_i^s against σ curve in Fig. 3. The calculated curve in Fig. 8 was obtained by changing σ_{i0}^s from 81.4 MPa to 80.0 MPa and $\sigma_i^s(0)$ from 3.0 MPa to 7.0 MPa. The value for $\sigma_{i\infty}$ was set equal to 14.0 MPa. Within the experimental uncertainty a nearly perfect fit can thus be obtained.

In Figs. 9 and 10 we have plotted the calculated values of the internal stress, as a function of time in Fig. 9, and as a function of remaining stress in Fig. 10. The solid line in each figure gives the internal stress corresponding to the calculated graph in Fig. 7, i.e. the slowness of the dislocation structure in adjusting to the decreasing stress is taken into consideration. The dotted lines give the internal stress in the secondary regime for the ideal case where the dislocation structure responds spontaneously to each load reduction. As is seen in Fig. 10, the sluggishness of the alloy results in internal stress values which are only a little higher than the ideal values which correspond to those of secondary creep. However, because the dependence of the strain rate on $(\sigma - \sigma_i)$ is to the power of 3.5, even a small increase in σ_i has a strong retarding effect on the relaxation. The consequence of this is a rather slow decrease in internal stress with time, as shown in Fig. 9. The upper graph in Fig. 9 represents the changes in internal stress during creep. For $t < t_p$ the graph is given by Equation 5. The curve has a knee at the transition point between primary and secondary creep. The reason for this is probably that Equation 5 is not exact (σ_i goes to infinitely with t). However, the curves in Fig. 9 give a fairly exact quantitative comparison between the internal stress during creep and stress relaxation. It is seen that early in the relaxation process the internal stress starts to deviate noticeably from the values valid for creep.

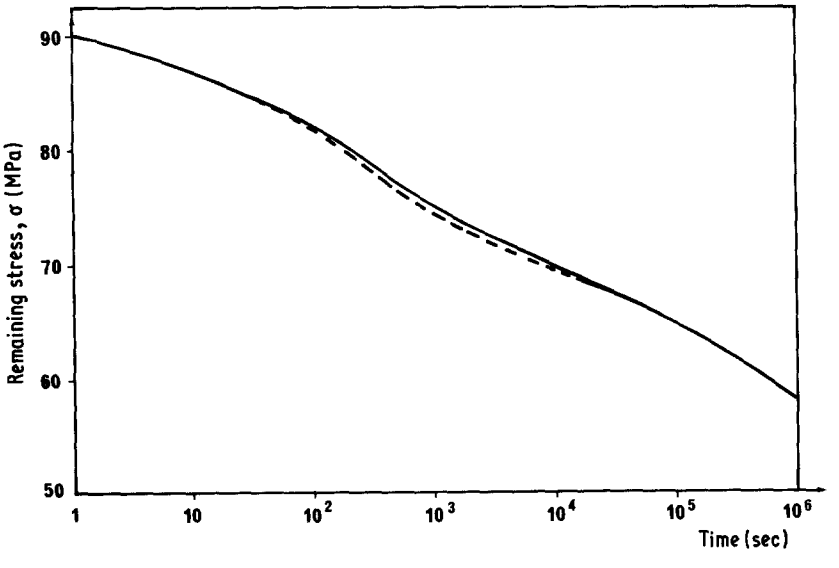

Figure 8 Experimental and calculated remaining stress as a function of time for AlSi12 at 100° C. (———) experimental, (- - -) calculated. $\sigma_{i0}^s = 80$ MPa, $\sigma_i^s(0) = 7$ MPa, $\sigma_{i\infty}^s = 14$ MPa.

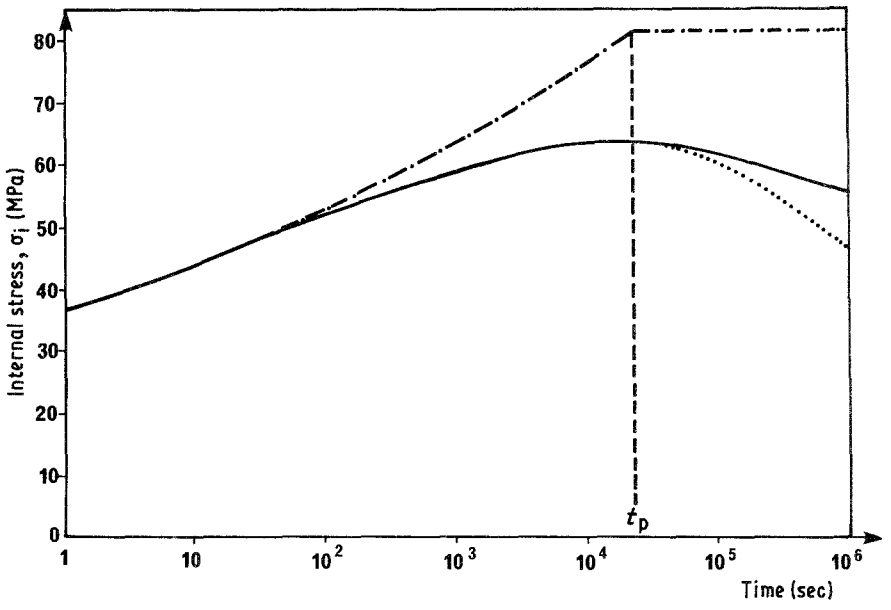

Figure 9 Internal stress as a function of time for creep and stress relaxation for AlSi12 at 100° C with σ_0 = 88.8 MPa. (———) stress relaxation, $\sigma_{i\infty}$ = 13 MPa; (···) stress relaxation, $\sigma_{i\infty}$ = $\sigma_i^s(0)$ = 3 MPa; (- · -) creep.

6. Discussion

The calculated curve in Fig. 6 fits the experimental curve very well in the primary region. Thus, at the beginning of the test when the dislocations are rearranging themselves they manage to adjust to the decreasing load. The reason for this might be the relatively low friction force which exists in the initial stage.

However, at the transition between the primary and secondary stage, an equilibrium dislocation structure has developed, and this structure is inherently more stable against a decreasing load. During the secondary stage, the internal stress therefore falls less than predicted by the internal stress values valid for creep. For the examined alloy the secondary internal stress is only slightly higher than the values predicted by creep. This is seen from Fig. 10, which by the dotted line gives the internal against applied stress for secondary creep, and by the solid line ($t > t_p$) gives the corresponding relationship for the calculated curve in Fig. 7. At the terminal stress level 58.5 MPa, the internal stress is only 1.5 MPa higher than the value for secondary creep. It thus seems that, due to the low relaxation rate at higher times (low remaining stress) the alloy is given enough time to develop a nearly equilibrium dislocation structure.

In pure aluminium there are fewer obstacles to dislocation motion than in AlSi12. The dislocation structure may therefore change more quickly in pure aluminium than in the alloy investigated. Pure aluminium may therefore be more capable than AlSi12 of producing a dislocation structure which is in equilibrium with the instantaneous remaining stress. If that is the case, the stress relaxation curve can be calculated solely on the basis of creep data. However for very complex alloys the dislocation structure may change very slowly after a load reduction. The internal stress in the secondary stage of stress relaxation may then end up way above the corresponding values for creep, and creep data will serve as a poor basis for stress relaxation calculations.

7. Conclusion

A semi-empirical model for stress relaxation has been developed by simulating the process mathematically by using the Evans–Harrison universal creep

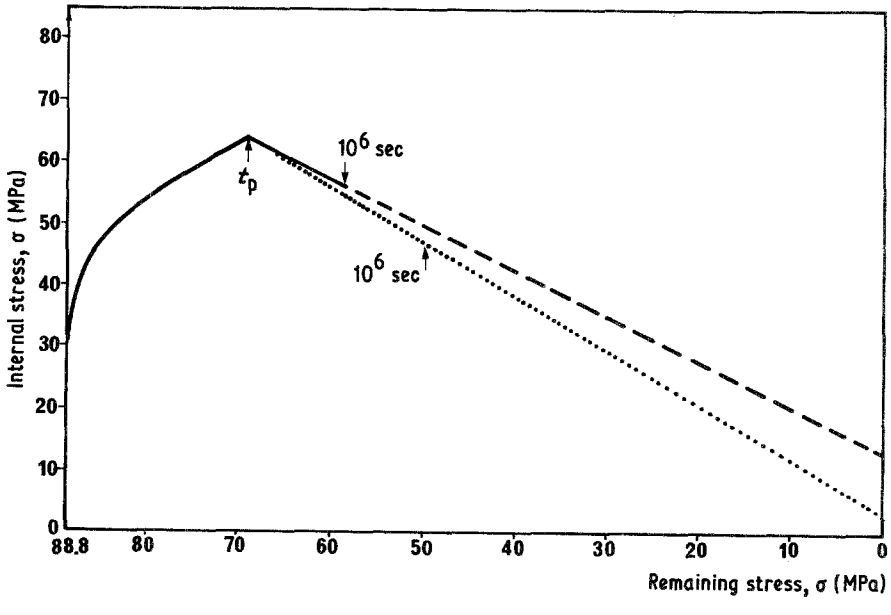

Figure 10 Internal stress as a function of remaining stress during stress relaxation of AlSi12 at 100° C. (- - -) $\sigma_{i\infty}$ = 13 MPa, (···) $\sigma_{i\infty}$ = $\sigma_i^s(0)$ = 3 MPa.

equation. In this model the relaxation life is divided into two stages in analogy with creep. The internal stress σ_i is treated as a complicated function of remaining stress and time. In the primary stage, σ_i is assumed to increase as the dislocation structure changes in the specimen. At the end of the primary stage, the dislocation structure is taken to be fully developed and equal to that for creep at the same instantaneous stress, giving a corresponding internal stress value. In the secondary stage, a reduction in the internal stress is assumed to succeed the reduction in the applied stress. The model was applied to the stress relaxation of AlSi12 (ÅSV 3001) at 100° C, and gave a very good fit for the primary stage. For the secondary stage a good fit was obtained only if the internal stress was assumed to fall less than predicted by creep values for the internal stress. This shows that during stress relaxation the dislocation structure is not given time enough to adjust completely to the falling stress.

References

1. H. HERØ, *Scripta Metall.* **9** (1975) 1121.
2. W. J. EVANS and G. F. HARRISON, *Met Sci.* **10** (1976) 307.
3. J. K. SOLBERG and H. THON, *Scripta Metall.* **19** (1985) 431.
4. W. J. EVANS and G. F. HARRISON, *Met. Sci.* **13** (1979) 641.

Received 4 February
and accepted 1 April 1985